

Effect of the upper mantle structure on the Moho geometry

TENZER, Robert^{1*} ; CHEN, Wenjin¹

¹School of Geodesy and Geomatics, Wuhan University

We investigate the effect of the lateral density structure within the upper (most) mantle on the Moho geometry. The gravimetric forward and inverse modeling methods are applied to determine the Moho depths using the gravity data corrected for major known anomalous density structures within the Earth crust. In our numerical experiment we compute and compare the Moho geometry determined using uniform and laterally varying models of the Moho density contrast. The laterally varying model of the Moho density contrast incorporates the information on the upper mantle lateral density structure taken from the CRUST1.0 global crustal model. For the uniform density contrast model, the constant value of the Moho density contrast is determined based on minimizing the spatial correlation between the gravity data and the Moho geometry. Except for the upper (most) mantle, the deeper heterogeneous mantle density structures including the core-mantle boundary zone are not taken into consideration due to the absence of a reliable 3-D density model of the whole mantle. The numerical results revealed that the consideration of the upper mantle density structure improves the fit of the gravimetric solution with the seismic Moho model.

Keywords: crust, density, gravity, mantle, Moho

Conductivity anisotropy of partial molten peridotite under shear deformation

ZHANG, Baohua¹ ; YOSHINO, Takashi^{1*} ; YAMAZAKI, Daisuke¹

¹Institute for Study of the Earth's Interior, Okayama Univ.

Recent ocean bottom magnetotelluric investigations have revealed a high-conductivity layer (HCL) with high anisotropy characterized by higher conductivity values in the direction parallel to the plate motion beneath the southern East Pacific Rise (Evans et al., 2005) and beneath the edge of the Cocos plate at the Middle America trench offshore of Nicaragua (Naif et al., 2013). These geophysical observations have been attributed to either hydration (water) of mantle minerals or the presence of partial melt. Currently, aligned partial melt has been regarded as the most preferable candidate for explaining the conductivity anisotropy because of the implausibility of proton conduction (Yoshino et al., 2006).

In this study, we report development of the conductivity anisotropy of partial molten peridotite in three directions parallel and normal to shear on the shear plane, and perpendicular to the shear plane as a function of time and shear strain. Starting samples were pre-synthesized partial molten peridotite (Fe-free and Fe-bearing systems), showing homogeneous melt distribution. The Fe-free and Fe-bearing partially molten peridotite samples were deformed in simple shear geometry at 1 GPa and 1523 and 1723 K, respectively, in a DIA-type apparatus with uniaxial deformation facility. Conductivity of the partially molten peridotite parallel to the shear direction was initially identical to that normal to shear. However, shear-parallel conductivity increased by more than one order of magnitude after the initiation of shear by piston advancement. Shear-parallel conductivity then stayed constant for the duration of the experimental run. On the other hand, conductivity normal to the shear direction on the shear plane remained constant, whereas conductivity perpendicular to the shear plane decreased gradually after initiation of shear and finally close to that of olivine. Conductivity difference between parallel and normal to shear direction reached one order, which is equivalent to that observed beneath asthenosphere. In contrast, such anisotropic behavior was not found in the melt-free samples, suggesting that development of the conductivity anisotropy was generated under shear stress.

Microstructure of the deformed partial molten peridotite shows partial melt tends to preferentially locate grain boundaries parallel to shear direction, and forms continuously thin melt layer sub-parallel to the shear direction, whereas apparently isolated distribution was observed on the section perpendicular to the shear direction. The resultant melt morphology can be approximated by tube like geometry parallel to the shear direction. This observation suggests that the development of conductivity anisotropy is caused by the realignment of partial melt (forming tube-like melt) parallel to shear direction in the silicate matrix.

In conclusion, the high anisotropy of conductivity in the direction of plate motion can be well explained by anisotropic interconnection of melt in partially molten rocks at the top of asthenosphere, but not hydration of nominally anhydrous minerals. Therefore, our results provide the direct experimental evidence for supporting these geophysically observed high-conductivity anisotropy at the LAB and verify the validity of partial melting hypothesis (Yoshino et al., 2006; Naif et al., 2013).

References

- Evans, R. L. et al. Geophysical evidence from the MELT area for compositional controls on oceanic plates. *Nature* 437, 249-252 (2005).
- Naif, S., Key, K., Constable, S. & Evans, R. L. Melt-rich channel observed at the lithosphere-asthenosphere boundary. *Nature* 495, 356-359 (2013).
- Yoshino, T., Matsuzaki, T., Yamashita, S. & Katsura, T. Hydrous olivine unable to account for conductivity anomaly at the top of the asthenosphere. *Nature* 443, 973-976 (2006).

Keywords: partial melting, asthenosphere, electrical conductivity, upper mantle, anisotropy, shear deformation

Surface-wave phase velocity maps of North America with inter-station waveform analysis

HAMADA, Kouta^{1*} ; YOSHIZAWA, Kazunori²

¹Graduate School of Science, Hokkaido University, ²Faculty of Science, Hokkaido University

The western United States encompasses a variety of tectonic features, including regions with east-west extension, volcanic areas and relatively stable cratonic regions.

In the last decade, the Transportable Array (USArray) has been installed throughout the U.S, and these waveform data have facilitated a variety of tomographic studies in this region using body and surface waves, and ambient noise analysis making the most of the high-density seismic network.

In this study, we have developed a new method of fully non-linear waveform fitting to measure inter-station phase velocities, using the Neighborhood Algorithm (NA) as a global optimizer. This algorithm searches for model parameters to fit two observed waveforms on a common great-circle path by perturbing the phase term of the fundamental-mode Love and Rayleigh waves. We have employed the reliability parameter, which represents how well the waveforms at two stations can be fitted in a time-frequency domain. This parameter is used as a data selection criterion for the subsequent step of phase velocity mapping.

The method has been applied to observed waveform data of the USArray from 2007 to 2010, and we could collect a large-number of phase speed data (over 45000 for Rayleigh and 15000 for Love) in a period range from 30 and 200 seconds, at short distances less than 1000 km. The phase velocity models for Rayleigh and Love waves indicate good correlation on large scales with the recent tomographic maps derived from different approaches for inter-station phase velocity measurements (Foster et al., 2013); e.g., significant slow velocity anomaly in volcanic regions in western Unites States and extremely fast anomaly in the cratonic region in the longer period range, which implies the robustness of such tectonic features as well as the validity of our new measurement technique. The current method can be expanded for the measurements of inter-station higher-mode phase velocities, which will be of great help in enhancing the vertical resolution of the 3-D shear wave models.

Keywords: surface wave, phase velocity, tomography, North America

Diffusion to dislocation creep transition in the upper mantle inferred from silicon grain boundary diffusion rates

FEI, Hongzhan^{1*}; KATSURA, Tomoo²; KOIZUMI, Sanae³; SAKAMOTO, Naoya⁴; HASHIGUCHI, Minako⁵; YURIMOTO, Hisayoshi⁵; YAMAZAKI, Daisuke¹

¹Institute for Study of the Earth's Interior, Okayama University, Japan, ²Bayerisches Geoinstitut, University of Bayreuth, Germany, ³Earthquake Research Institute, The University of Tokyo, Japan, ⁴Isotope Imaging Laboratory, CRI, Hokkaido University, Japan, ⁵Department of Natural History Sciences, Hokkaido University, Japan

The majority of the dynamical processes in the upper mantle are controlled by creep of minerals. Dislocation creep causes non-Newtonian viscosity and seismic anisotropy whereas diffusion creep causes Newtonian viscosity and no seismic anisotropy. Determination of deformation mechanism in the upper interior is thus essential to understand mantle dynamics. Previous deformation studies on olivine suggested that the shallow regions of the upper mantle should be dominated by dislocation creep and the deeper regions dominated by diffusion creep [Karato, 1992; Karato and Wu, 1993; Hirth and Kohlstedt, 2003]. However, recent study [Fei et al., 2013] demonstrated that those deformation experiments largely misunderstood the creep rate due to the experimental difficulties. Since the creep of olivine is controlled by silicon diffusion, we measured silicon grain-boundary diffusion coefficient in Mg-olivine aggregates as a function of pressure, temperature, and water content. The activation energy, activation volume, and water content exponent are found to be 240-260 kJ/mol, 1.8 ± 0.2 cm³/mol, and 0.22 ± 0.05 , respectively. Together with the silicon lattice diffusion data [Fei et al., 2012; 2013], our results predict the diffusion to dislocation creep transition in the upper mantle, which is in contrast with the previously considered model. In the asthenosphere, dislocation creep should dominate because of the high temperature. In the lithosphere, diffusion creep dominates in shallow regions and dislocation creep dominates in deeper parts. The seismic anisotropy jumps at mid-lithosphere discontinuity beneath continents and at Gutenberg discontinuity beneath oceans are caused by the transition from diffusion to dislocation creep. The weak anisotropy in cold lithospheres could be attributed to the fossil anisotropy formed at the spreading ridges. Dominance of diffusion creep in upper lithosphere accounts for the Newtonian rheology suggested by postglacial rebound.

Fei et al., *EPSL* **345**, 95-103 (2012).

Fei et al., *Nature* **498**, 213-215 (2013).

Hirth and Kohlstedt, *Geophys. Monogr.* **138**, 83-105 (2003).

Karato, *JGR* **19**, 2255-2258 (1992).

Karato and Wu, *Science* **260**, 771-778 (1993).

Keywords: diffusion creep, dislocation creep, upper mantle, silicon, grain boundary diffusion, deformation mechanism

Aluminum incorporation into phase A - a new hydrous silicate in the deep upper mantle

CAI, Nao^{1*} ; INOUE, Toru¹ ; FUJINO, Kiyoshi¹ ; OHFUJI, Hiroaki¹ ; KURIBAYASHI, Takahiro² ; YURIMOTO, Hisayoshi³

¹Geodynamics Research Center, Ehime University, ²Institute of Mineralogy, Petrology and Economic Geology, Graduate School of Science, Tohoku University, ³Division of Earth and Planetary Sciences, Hokaido University

A new aluminum bearing hydrous silicate was found in the experiments under the deep upper mantle conditions, using phase A ($\text{Mg}_7\text{Si}_2\text{O}_8(\text{OH})_6$) and $\text{Al}(\text{OH})_3$ as the starting materials. Using electron probe micro analysis (EPMA) and secondary ion mass spectrometry (SIMS), the composition was determined to be very close to $\text{Mg}_{5.5}\text{AlSi}_2\text{O}_8(\text{OH})_6$, which contained about 12 wt % of water. Almost pure phase was obtained in the subsequent experiments. The powder x-ray diffraction pattern and transmission electron diffraction patterns showed a hexagonal structure, with an abnormal large c axis. This new phase has similar stability region with phase A. At lower pressure and higher temperature, it breaks down into Chondrodite + Garnet + Brucite + Fluid, while at higher pressure and higher temperature, it breaks down into Al-superhydrous phase B + Garnet + Brucite + Fluid.

Besides, present study shows that phase A coexists with this aluminum bearing hydrous phase, with a small amount of aluminum (<1 wt%) incorporated into phase A structure, which predicts that phase A can preserve only trace of aluminum.

According to Inoue's unpublished data, aluminum can easily incorporate into some dense hydrous magnesium silicates and form aluminum bearing hydrous phases such as phase B, superhydrous phase B, and even perovskite. However, rather than aluminum bearing phase A, the present study shows a small amount of aluminum incorporation into phase A structure, and an appearance of a new aluminum bearing hydrous phase, with the composition very similar to phase A but structure very different from it. Further investigations are needed to clarify these two phases.

Keywords: Phase A, Aluminum incorporation, hydrous phase, upper mantle

Changbai intraplate volcanism and deep earthquakes in Northeast Asia

ZHAO, Dapeng^{1*} ; TIAN, You¹

¹Tohoku University, Department of Geophysics

The origin of the intraplate volcanoes in Northeast Asia is considered to be associated with upwelling of hot and wet asthenospheric materials in the big mantle wedge above the stagnant Pacific slab in the mantle transition zone. Among these intraplate volcanoes, Changbai is the largest and most active one, and very deep earthquakes (500-600 km depths) in the Pacific slab under East Asia occur ~300 km to the east of the Changbai volcano. Integrating the findings of geophysical, geochemical and petrologic studies so far, we suggest a link between the Changbai volcanism and the deep earthquakes in the Pacific slab. Many large shallow earthquakes occurred in the Pacific plate in the outer-rise areas close to the oceanic trench, and seawater may enter down to the deep portion of the oceanic lithosphere through the active normal faults which generated the large outer-rise earthquakes. The seawater or fluids may be preserved in the active faults even after the Pacific plate subducts into the mantle. Many large deep earthquakes are observed that took place in the subducting Pacific slab under the Japan Sea and the East Asian margin. At least some of the large deep earthquakes are caused by the reactivation of the faults preserved in the subducting slab, and the fluids preserved in the faults within the slab may cause the observed non-double-couple components in the deep earthquake faulting. The fluids preserved in the slab may be released to the overlying mantle wedge through the large deep earthquakes. Because large deep earthquakes occur frequently in the vicinity of the Changbai volcano, much more fluids could be supplied to this volcano than other areas in Northeast Asia, making Changbai the largest and most active intraplate volcano in the region.

Reference

Zhao, D., Y. Tian (2013) Changbai intraplate volcanism and deep earthquakes in East Asia: A possible link? *Geophys. J. Int.* 195, 706-724.

Keywords: volcanoes, deep earthquakes, Asia, slab

Semiconductor diamond heater (SCD): An innovation for ultrahigh temperature experiments in the Kawai cell

XIE, Longjian^{1*} ; ITO, Eiji¹ ; YONENDA, Akira¹

¹Institute for Study of the Earth Interior , Okayama University

We developed the semi-conductor diamond heater in the Kawai high pressure cell. The starting material of the semi-conductor diamond heater is born(B)-doped burned-graphite. We succeeded to improve the machinability of the B-doped burned-graphite by decreasing porosity. Following is the motivation and the background of the semi-conductor diamond heater project.

It is important to generate extremely high temperature (~ 3000 °C) in a large sample volume ($\sim 0.1\text{mm}^3$) in the Kawai apparatus. X-ray transparency is also desirable for in-situ synchrotron analysis. However, any traditional heater used in the Kawai apparatus so far does not satisfy the both requirements simultaneously.

Semiconductor diamond is a candidate material to generate temperatures higher than 3000 °C with low x-ray absorption. Anton Shatskiy (2009) have generated a temperature of 3500 °C by using the semiconductor diamond heater in a large-volume Kawai-type high-pressure apparatus, although their temperature measurement is questionable from a viewpoint of the power-temperature relation. Furthermore, their semi-conducted diamond heater, made of boron and graphite powders, was not machinable and difficult to control the temperatures. It often became unstable at around 1000~1300 °C and impossible to generate higher temperature.

Systematic experiments have done to improve the performance of the semiconductor heater. We used a machinable block of graphite contain 3 wt.% boron as the starting material for the semi-conductor diamond heater. The graphite-diamond transformation started at ~ 1000 - 1200 °C at 15 GPa in the Kawai apparatus. After the transformation, we stably generated temperature to 2000 °C. Activation energy of B-doped diamond is about 0.1 eV, which is much lower than that of pure diamond (5.45eV).

References:

Anton Shatskiy, Daisuke Yamazaki, Guillaume Morard, Titus Cooray, Takuya Matsuzaki et al. , Review of Scientific Instruments 80, 023907 (2009).

Keywords: Semiconductor Diamond Heater, Ultrahigh Temperature, Kawai Cell

Recent Global Tomography Models: Where are We Heading for?

TAKEUCHI, Nozomu^{1*}

¹Earthquake Research Institute, University of Tokyo

Many high-resolution global tomography models have been obtained and we now have consensus about overall features of 3-D heterogeneous structure in the Earth. Majority of models have been obtained by using conventional ray theory which assumes that scale length of lateral heterogeneities is sufficiently large compared with wavelength of seismic waves analyzed.

Primary efforts in recent studies appear to introduce better theories to overcome resolution limits caused by the above-mentioned assumption. The efforts include delay time tomography with finite frequency kernels (e.g., Montelli et al. 2004, *Science*; Obayashi et al. 2013, *GRL*) and waveform tomography with 2-D (e.g, Li and Romanowicz 1996, *GJI*, Panning and Romanowicz 2004, *Science*) or 3-D (e.g, Takeuchi 2007, *GJI*; Takeuchi 2012, *EPSL*) finite frequency kernels. Waveform tomography with further better theories is also becoming feasible (e.g., Lekic and Romanowicz 2011, *GJI*; French et al. 2013, *Science*).

In this presentation, I want to propose another direction to improve resolution: use of a new type of dataset. I will propose to use incoherent part of seismic signals (i.e., scattering waves or coda waves). Scattering waves are sensitive to heterogeneities whose scale length is comparable with wavelength of seismic waves analyzed. Use of such waves therefore should provide new information beyond resolution limit of ray theory. At the time of the presentation, I plan to show feasibility and examples of such analyses to reveal distribution of smaller scale heterogeneities in the subduction zone around Japan.

Keywords: tomography, scattering wave, seismology

Lattice preferred orientation of stishovite in deformation experiment

XU, Fang^{1*}; YAMAZAKI, Daisuke¹; TSUJINO, Noriyoshi¹

¹ISEI, Okayama University

Seismic observations reveal strong negative anisotropy ($V_{SV} > V_{SH}$) at around 550 km depth in the lower part of mantle transition zone (Visser et al., 2008). The mantle tomography indicates the obvious association of this negative anisotropy with the subduction zones (Panning and Romanowicz., 2006). The observed anisotropy can be caused by lattice preferred orientation (LPO) of constituting material when the material is elastically anisotropic. Majorite and ringwoodite, which are the dominant minerals in this region, are nearly isotropic (Chai et al., 1997; Weidner et al., 1984). On the other hand, stishovite, which may occur in significant amounts in this region derived from the delaminated subducting basaltic layer (Karato et al., 1997) and continental crust (Kawai et al., 2012), shows strong elastic anisotropy (V_{SV}/V_{SH} is as large as 150%) indicated by the acoustic velocities study (Yoneda et al., 2012) on single crystal of stishovite. Therefore, the LPO of stishovite has a high potential to interpret the seismic anisotropy in the lower part of the transition zone and indicate the geometry of mantle flow.

To investigate the LPO of stishovite, deformation experiments on stishovite were conducted in both simple shear and uni-axial geometry. We prepared starting material of polycrystalline stishovite with grain size of $\sim 10 \mu\text{m}$ at 12 GPa and 1450 °C in a Kawai-type high-pressure apparatus. Then deformation experiments were carried out at 12 GPa and 1600 °C by Kawai-type apparatus for tri-axial deformation (KATD installed at Tokyo Institute of Technology) and deformation-DIA apparatus (SPEED-Mk. II installed at SPring-8). Sintered diamond piston was used in the uni-axial deformation experiment. Shear strain was ~ 1.0 estimated from the rotation of platinum strain maker after deformation. From the change of sample length, uni-axial tension and compression strain were 0.4 and 0.1 respectively. The microstructure and crystallographic orientation of the deformed samples were investigated by SEM with EBSD.

The EBSD results reveal that the [001] direction of stishovite tends to be parallel to the shear direction. (100) plane, though not so obvious, tends to parallel to the shear plane. The slip system is consistent with rutile TiO_2 (Blanchin and Faisant., 1979), which has the same structure with stishovite. The calculated seismic anisotropy indicates a fast shear wave along shear direction. Polarization anisotropy reported by Visser et al. (2008) can be attributed by a vertical flow and LPO of stishovite in the transition zone. The negative anisotropy along subduction zones in Panning and Romanowicz. (2006) indicates the type A slabs (slabs which penetrate directly into the lower mantle without much deflection in the transition zone) (Karato et al., 2001).

Keywords: stishovite, deformation, LPO

Phase transitions and mineral chemistry in pyrolite at 1600-2200C across 660-km seismic discontinuity

ISHII, Takayuki^{1*} ; KOJITANI, Hiroshi¹ ; AKAOGI, Masaki¹

¹Department of chemistry, Gakushuin University

It is widely accepted that pyrolite is a model rock which represents the chemical composition of the Earth's upper mantle. Because the post-spinel transition in pyrolite occurs at about 23 GPa along mantle geotherm (e.g. Litasov et al. 2005), it has been accepted that the transition is responsible for the seismic 660-km discontinuity. Slow velocity anomalies by global seismic tomography which may indicate mantle upwelling have been found in the transition zone and the lower mantle, and these regions are higher in temperature than average mantle. To elucidate the origin and dynamics of the mantle plume, informations on phase relations in pyrolite are essential. However, few investigations on phase relations in pyrolite have been made at hot-plume temperatures (1800-2200C) (Hirose, 2002; Nishiyama and Yagi, 2003). In this study, we demonstrated detailed phase equilibrium experiments in pyrolite composition at hot plume conditions.

The starting material was prepared as the oxide mixture in pyrolite composition after McDonough and Sun (1995) excluding minor components (MnO, K₂O and P₂O₅). Quench experiments were made at about 20-28 GPa and 1600-2200C for 2-10 hours using a Kawai-type 6-8 multianvil high-pressure apparatus at Gakushuin University. The starting material was packed with pressure calibrants (MgSiO₃ and pyrope) in a Re multi-sample capsule. A LaCrO₃ heater and a W5%Re-W26%Re thermocouple were inserted in a Cr₂O₃-doped MgO pressure medium. Phases of recovered samples were identified with microfocus-Xray diffractometer and SEM-EDS.

The mineral assemblages of MgSiO₃-rich perovskite (Mpv) + magnesiowustite (Mw) + garnet (Gt) + CaSiO₃-perovskite (Cpv) and Mpv + Mw + Cpv at 1600-2200C are stable at pressure range of 22-24 GPa and above 24 GPa, respectively. The mineral assemblage of ringwoodite (Rw) + Gt + Cpv at 1600C changes to that of Rw + Mw + Gt + Cpv at 1800-2000C, and Rw disappears perfectly above 2200C. From mass balance calculation of analyzed compositions of the phases, we found that Gt content increases with increasing temperature before and after formation of Mpv. We also calculated the densities in pyrolite at each temperature. The density of average pyrolite mantle (1600C) is higher than pyrolite plume (1800-2200C) across 660-km discontinuity due to increase in Gt content with increasing temperature. Therefore, we conclude that hot-plume ascending nearby 660-km discontinuity has positive buoyancy by the phase transitions.

Keywords: post-spinel transition, 660-km seismic discontinuity, mantle plume, pyrolite, post-garnet transition

Elastic properties of delta-AIOOH under high-pressure: Implications for high V_S anomaly in the mantle transition zone

MASHINO, Izumi^{1*}; MURAKAMI, Motohiko¹; OHTANI, Eiji¹

¹Faculty of Science, Tohoku University

delta-AIOOH is a high-pressure polymorph of diaspore (alpha-AIOOH) and boehmite (gamma-AIOOH) (Suzuki *et al.*, 2000). Since delta-AIOOH is identified to be stable from 20 to 120 GPa, and temperatures up to 2300 K, this phase is considered to be a possible carrier and reservoir of water in subducting cold slab into the deep mantle (Ohtani *et al.*, 2001; Sano *et al.*, 2004; 2008). In order to investigate the effect of composition on seismic velocities in subducting slab, it is important to measure the elastic properties of delta-AIOOH at high pressure.

We have conducted high-pressure acoustic-wave velocity measurements of delta-AIOOH using Brillouin spectroscopy and also explored the chemical bonding of delta-AIOOH by Raman spectroscopy at high pressure in a diamond anvil cell. We obtained sharp peaks from transverse acoustic mode (V_S) of delta-AIOOH over the entire pressure range explored up to a pressure of 89 GPa. The peaks from longitudinal acoustic mode (V_P) of delta-AIOOH were masked by the diamond shear acoustic modes from 35 GPa. The pressure dependence of the aggregate velocities for the delta-AIOOH at 300 K suggests that the hydrogen-bonding symmetrization with the space group changes from $P2_1nm$ to $Pnmm$ occurs during compression above 7 GPa. The shear and adiabatic bulk moduli and their pressure derivatives at zero pressure were determined to be $K_0 = 192.2(8)$ (GPa), $G_0 = 158.8(3)$ (GPa), $(dK/dP)_0 = 3.63(6)$, and $(dG/dP)_0 = 1.35(6)$ for the pressures above 15 GPa. Raman spectroscopic measurements have shown that the B_1 mode frequencies of $P2_1nm$ disappeared around 6 GPa and A_g mode frequencies of $Pnmm$ appeared above 5.6 GPa, which also indicates the hydrogen-bonding symmetrization around 6 GPa. These results indicate that delta-AIOOH becomes harder by the hydrogen-bonding symmetrization and probably exists as a phase ($Pnmm$) with the symmetric hydrogen bonding in the mantle transition zone and lower mantle.

Shear wave velocities for delta-AIOOH are larger than those of hydrous wadsleyite (by 30 %), hydrous ringwoodite (by 29 %), and majorite (by 29 %). Those of delta-AIOOH are approximately 7 % below those of stishovite. The delta-AIOOH phase thus found to be one of the hardest phases compared to the minerals of mantle transition zone. The existence of delta-AIOOH may contribute to the cause of high V_S and V_P anomalies. Shear velocities for sediment containing delta-AIOOH phase are larger than those of pyrolite (by 10 %) and MORB (by 5 %). The subducting slabs often stagnate at the transition zone before reaching the lower mantle. Particularly beneath Korean peninsula, there is a high V_S anomaly (~2 %) in the lower part of the transition zone (Zhang *et al.*, 2012). The seismic data under the eastern part of northeast China (NEC) also indicates a slight positive anomaly of V_S (~1 %), but the V_S value observed around 600 km depth under NEC is ~1 % lower than that beneath Korea. We explain the difference in the V_S anomalies beneath the NEC and Korea by the amount of sediment containing the delta-AIOOH phase and the stagnating duration. If sediments stagnate at the transition zone before reaching the lower mantle in this region, we can estimate that the higher V_S anomaly (~1 %) than NEC would correspond to sediments with 13.4 vol% in stagnant slab. The average oceanic crust subduction rate is estimated to be about 8 cm/yr around Japan. Assuming this estimated rate of subduction, the slab stagnation has lasted for at least 30 million years.

Keywords: delta-AIOOH, Brillouin scattering, Raman spectroscopy, subducting slab, high pressure

Mechanisms of ultra-deep earthquakes ($h > 660\text{km}$) in a slab penetrating the 660-km discontinuity

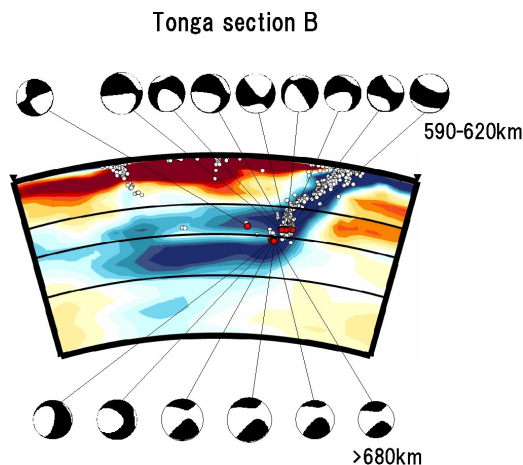
FUKAO, Yoshio^{1*}; OBAYASHI, Masayuki¹; YOSHIMITSU, Junko¹

¹IFREE/JAMSTEC

Recent mantle tomography has begun to reveal the characteristic differences between the deep hypocentral distributions associated with stagnant slabs and those associated with penetrating slabs (e.g., Fukao and Obayashi, 2014). We here show that there are differences in focal mechanism as well. Mechanisms of deep shocks within tomographically imaged stagnant slabs (typically in Bonin and Tonga) are characterized by horizontal compression (e.g., Bonnardot et al., 2009). Those within tomographically imaged penetrating slabs (typically in Java and Tonga) are characterized by very steeply dipping compressional axes (e.g., Alpert et al., 2010).

The deepest seismicity is especially active in Tonga, where many shocks occur at depths greater than 660km. Such ultra-deep shocks show in general very unusual mechanisms, typified by nearly vertical tensional axes with a large amount of CLVD component, as demonstrated in Figure 1 (Mechanisms viewed from the side). This figure also shows a remarkable contrast of mechanisms of deepest shocks just above and below the 660km depth. The source region of the ultra-deep shocks ($h > 660\text{km}$) is underlain by the greatly deepened post-spinel phase boundary (Niu and Kawakatsu, 1995) so that the source region is at the pre-spinel state while the underlying portion is at the post-spinel state. This situation along with contortion of the slab associated with its interaction with the post-spinel phase boundary (e.g., Cizkova and Bina, 2013) may explain the mechanism change across the 660km depth as observed in Figure 1. We explore the finer velocity structure and hypocentral distribution in the source region by a technique of differential travel time tomography.

Keywords: mantle dynamics, tomography, deep earthquakes



A pyrolitic lower mantle with $(\text{Mg,Fe}^{3+})(\text{Si,Al}^{3+})\text{O}_3$ perovskite

WANG, Xianlong^{1*} ; TSUCHIYA, Taku¹

¹GRC, Ehime University and ELSI, Tokyo Institute of Technology

To better understand the Earth's lower mantle (LM), thermodynamic properties (TDPs) of LM minerals with Fe and Al dopant should be illustrated more clearly. We have so far reported the TDPs of Fe-bearing MgO, MgSiO₃ perovskite (Pv) and post perovskite. [1-4] We furthermore study the TDPs of Fe- and Al-bearing Pv, where the internally consistent LSDA+*U* method and the lattice dynamics method are applied. Two spin states, high (HS) and low spin state, two substitution sites, Mg and Si site, and several possible distribution configurations are considered. In the LM pressure range, HS Fe³⁺ substituted at the Mg site with Al³⁺ at the adjacent Si site (Fe-Al pair) is the most stable configuration and tends to distribute homogeneously in LM. Furthermore, negative frequency cannot be observed in the Fe-Al pair-bearing Pv, and Al contributes to middle frequency while Fe mainly to low part due to its heavy mass. This indicates that the Fe-Al pair is vibrationally stable. Incorporation of the pair for geophysically relevant concentrations can increase volume of Pv a little and has marginal effects on the TDPs of Pv except for thermal expansivity and Gruneisen parameter. Simulated densities, adiabatic bulk moduli, and bulk sound velocities show that a composition close to pyrolite is accountable for the reference Earth model.

References:

- [1] A. Metsue, and T. Tsuchiya, J. Geophys. Res. 116, B08207 (2011).
- [2] A. Metsue, and T. Tsuchiya, Geophys. J. Int. 190, 310 (2012).
- [3] H. Fukui, T. Tsuchiya, and A. Q. R. Baron, J. Geophys. Res. 117, B12202 (2012).
- [4] T. Tsuchiya, and X. Wang, J. Geophys. 118, 83 (2013).

Keywords: First-principles method, Internally consistent LSDA+*U*, Perovskite, Thermodynamic properties, Pyrolite

Linear analysis on the onset of thermal convection of highly compressible fluids

KAMEYAMA, Masanori^{1*}

¹GRC, Ehime University

A series of linear stability analysis was performed on the onset of thermal convection in a highly compressible fluid, in order to study the fundamental nature of mantle convection of massive super-Earths in the presence of strong adiabatic compression. We consider the temporal evolution (growth or decay) of an infinitesimal perturbation superimposed to a highly compressible fluid which is in a hydrostatic (motionless) and conductive state in a basally-heated horizontal layer. As a model of pressure-dependence in material properties, we employed an exponential decrease in thermal expansivity and exponential increase in (reference) density with depth. The linearized equations for conservation of mass, momentum and internal (thermal) energy are numerically solved for the critical Rayleigh number as well as the vertical profiles of eigenfunctions for infinitesimal perturbations. The above calculations are repeatedly carried out by systematically varying (i) the dissipation number which measures the effect of adiabatic compression, (ii) the temperature at the top surface and (iii) the magnitude of pressure-dependence in thermal expansivity and reference density.

Our analysis demonstrated that the onset of thermal convection is strongly affected by the adiabatic compression, through modulating the static stability of thermal stratification in the fluid layer. For sufficiently strong adiabatic compression where a sufficiently thick “stratosphere” of stable stratification develops in the layer, for example, the critical Rayleigh number explosively increases with the dissipation number. The explosive changes in the critical Rayleigh number are associated with drastic decreases in the length scales of perturbations both in vertical and horizontal directions. In particular, for very strong adiabatic compression, the vertical motion of fluid is significantly suppressed in a thick “stratosphere”, which narrows the incipient convection in a thin sublayer of unstable thermal stratification. In addition, when the effect of adiabatic compression is extremely strong so that the thermal stratification becomes stable in the entire layer, no perturbation is allowed to grow with time regardless of the Rayleigh number and/or the horizontal wavelength. We also found that the effect of adiabatic compression becomes prominent for higher temperature at the top surface of the fluid layer. These findings may imply the crucial importance of adiabatic compression in understanding the dynamics and evolution of the mantles of massive super-Earths, particularly for those orbiting their parent stars very closely.

Keywords: super-Earths, mantle convection, adiabatic compression, thermal expansivity

In Situ observation of the Segregation Process of Molten Iron from Partially Molten Silicate using X-ray Radiography

YAGI, Takehiko^{1*} ; GOTOU, Hirotada² ; IIZUKA, Riko¹ ; SUZUKI, Akio³

¹Geodynamics Research Center, Ehime University, ²Institute for Solid State Physics, University of Tokyo, ³Department of Earth Science, Tohoku University

We have made in situ observation of the segregation process of molten iron from partially molten silicate at 5 GPa and 1800 K using X-ray radiography. Earth's core is believed to have formed by the similar process in the early stage of Earth formation. Although two measure mechanisms, "rain fall" and "percolation", have been proposed for this process, experimental results are still quite controversial. Most of the previous works were made either by the texture analysis of the quenched and recovered sample or by the electrical conductivity measurement. In the present study, an uniform mixture of the powders of Mg(OH)₂, SiO₂, and Fe was compressed to 5 GPa at room temperature and then X-ray tomography observation was made with increasing temperature up to 1800 K. Addition of H₂O component into silicate-iron system reduces the melting temperature of both silicate and iron considerably. The dynamical process of the formation of iron ball at the bottom of the sample chamber was clearly observed. It was proved that this technique is quite useful to study such process in detail.

Keywords: core formation process, molten iron, x-ray, high pressure and temperature

Influence of majorite on mantle convection

ICHIKAWA, Hiroki^{1*} ; KAMEYAMA, Masanori² ; SENSU, Hiroki³ ; KAWAI, Kenji⁴ ; MARUYAMA, Shigenori⁵

¹GRC, Ehime University and ELSI, Tokyo Institute of Technology, ²Geodynamics Research Center, Ehime University, ³Planetary Exploration Research Center, Chiba Institute of Technology, ⁴Department of Earth and Planetary Sciences, Tokyo Institute of Technology, ⁵Earth-Life Science Institute, Tokyo Institute of Technology

Influence of MgSiO_3 majorite on the mantle convection has been investigated by using numerical simulations. According to a first principles study (Yu et al., 2011), wadsleyite decomposes to an assemblage of majorite plus periclase with a large negative Clapeyron slope. Since stability field of majorite is limited at high temperature, downwellings are considered to be unaffected by this phase boundary. On the contrary, the upwelling plumes may be significantly modified by this phase boundary. The asymmetry on upwelling and downwelling caused by the phase transitions may induce strong effects on the thermal evolution and the thermal structure of the mantle.

In this study, we performed 2-D numerical simulations on thermal convection of the mantle incorporating majorite stability field. According to our numerical results, very hot upwelling plumes are strongly influenced by the phase transitions related to majorite. The dynamics of these upwellings are controlled by the release and the absorption of latent heat induced by the transitions as well as interruption of currents due to the large negative Clapeyron slope of the transition between wadsleyite and majorite plus periclase.

Keywords: Mantle convection, Majorite, Phase transition

Rapid lateral variation of P-wave velocity at the base of the mantle beneath the Western Pacific

TANAKA, Satoru^{1*} ; KAWAKATSU, Hotoshi² ; OBAYASHI, Masayuki¹ ; NECESSARRAY, Project team²

¹JAMSTEC, ²ERI, Univ. Tokyo

We examine P-wave velocity structure at the base of the mantle beneath the Western Pacific, where is the western edge of the Pacific Large-Low Velocity Province (LLVP), by using high-quality seismograms that are provided by the NECESSArray project. Forward modeling with the reflectivity method is conducted to explain the variation of P-wave travel times as function of epicentral distance near the core shadow zone after station and ellipticity corrections are applied. Additionally PcP-P travel times are also examined to enlarge the survey area. As a result, a rapid variation of P-wave velocity structure at the base of the mantle is detected. Thin (10 to 60 km thickness) and very low velocity (-2 to -6 %) layers at the base of the mantle are intersected with a 100 km thickness and high velocity (+3%) layer, and a slightly fast layer exists at the north of the region with the thin and low velocity layers. Their spatial separations are typically several hundred kilometers and it would be difficult to explain by only a thermal effect. These observations suggest that very complicated thermo-chemical reactions occur near the edge of Pacific LLVP.

Keywords: P-wave velocity, the base of the mantle, the Western Pacific

Methods for inversion of body-wave waveforms for localized three-dimensional seismic structure and an application to D''

KAWAI, Kenji^{1*} ; KONISHI, Kensuke² ; GELLER, Robert J.³ ; FUJI, Nobuaki⁴

¹Department of Earth and Planetary Sciences, Tokyo Institute of Technology, ²School of Earth and Environmental Sciences, Seoul National University, ³Department of Earth and Planetary Science, Graduate School of Science, University of Tokyo, ⁴Institut de Physique du Globe de Paris

We formulate the inverse problem of waveform inversion for localized 3-D seismic structure, computing partial derivatives of waveforms with respect to the elastic moduli at arbitrary points in space for anisotropic and anelastic media. In this study we minimize computational requirements by using the Born approximation with respect to a laterally homogeneous model, but this is not an inherent limitation of our approach. We solve the inverse problem using the conjugate gradient (CG) method, using Akaike's Information Criterion (AIC) to truncate the CG expansion. We apply our method to invert for three-dimensional shear wave structure in the lowermost mantle beneath Central America using a total of 2154 waveforms at periods from 12.5 to 200 s recorded at stations near the Pacific coast of North America for 29 deep and intermediate-depth events beneath South America. The resulting model shows lateral heterogeneity in the E-W direction which may be associated with a subducted cold slab surrounded by hotter materials with slower velocities. Various tests show that our model is robust.

Keywords: Lowermost mantle, Waveform inversion, Farallon plate

A magnetic probe into Earth's core and deep-mantle dynamics

SAKURABA, Ataru^{1*}

¹Department of Earth and Planetary Science, University of Tokyo

It is widely recognized that Earth's core dynamics is an important research subject in understanding the past, present and future states of our planet, firstly because the metallic core is a vast domain accounting for one thirds of Earth's mass and plays a significant role in thermal history, and secondly because it dynamically generates the main geomagnetic field that has historically been observed for several hundred years and geologically recorded in rocks since more than a billion years ago. This review attempts to cover this subject with an attention to general questions: how geomagnetic-field data can be used to advance the deep-Earth science, and what theoretical progresses have been made and could be made. I will deal with some of the following particular topics: (1) various driving sources of convection, such as thermal and compositional buoyancy and inertial forcing (e.g., luni-solar precession); (2) a dynamo without a solid inner core; (3) a dynamo that operates in a part (e.g., an inner part) of the outer core; (4) sensitivity of the geomagnetic field structure (e.g., dipolarity), intensity, and time variations (e.g., reversal frequency) to the above mentioned various parameters.

Relationship between sound velocity and density of liquid alloy under pressure

TERASAKI, Hidenori^{1*}; NISHIDA, Keisuke²; URAKAWA, Satoru³; KUWABARA, Souma¹; TAKUBO, Yusaku¹; SHI-MOYAMA, Yuta¹; UESUGI, Kentaro⁴; TAKEUCHI, Akihisa⁴; SUZUKI, Yoshio⁴; KONO, Yoshio⁵; HIGO, Yuji⁴; KONDO, Tadashi¹

¹Osaka Univ., ²Univ. Tokyo, ³Okayama Univ., ⁴JASRI, ⁵HPCAT

It is important to understand the relationship between sound velocity and density of liquid Fe-alloys under high pressure for obtaining a constraint of the composition of the molten outer core from observed seismic data. We have studied a relationship between sound velocity and density of liquid alloy based on simultaneous measurement of these properties under high pressure and high temperature. Sound velocity was measured using ultrasonic pulse-echo overlapping method and density was measured employing X-ray absorption method combined with X-ray tomography technique. The measured P-wave velocity and density of liquid Ni₉₀S both increase with pressure. From these data, adiabatic bulk modulus (K_{S0}) of the liquid sample can be well constrained to 29 GPa. It is note that the measured P-wave velocity is found to increase linearly with increasing density. This result provides an important issue in terms of Birch's law for liquid material.

Keywords: Sound velocity, density, liquid, high pressure

Magnetic-Coriolis waves in convection-driven dynamos: Implications for geomagnetic westward drift

HORI, Kumiko^{1*} ; JONES, Chris² ; WICHT, Johannes³ ; SHIMIZU, Hisayoshi¹

¹Earthquake Research Institute, University of Tokyo, ²University of Leeds, UK, ³Max-Planck Institute for Solar System Research, Germany

A prominent feature of the geomagnetic secular variation is the westward motion of the non-dipole part of the field, which is significant in the Atlantic hemisphere with timescales of a few hundred years. Potential mechanisms to account for longitudinal geomagnetic drifts are advection due to large-scale zonal flows in the Earth's core as well as propagation of rotating magnetohydrodynamic (MHD) waves, particularly of slow Magnetic-Coriolis (MC) Rossby waves. More commonly the westward motion is thought to reflect zonal flow advection, an assumption that is used when inverting the secular variation signal for the flow at the top of the core. However, recent geodynamo simulations have successfully reproduced longitudinal magnetic drifts and some authors reported that the drift is at least partly a wave propagation.

To assess to what extent waves could play a role in geomagnetic drift, we explore nonlinear simulations of convection-driven MHD dynamos in rotating spherical shells. By performing a tempo-spatial spectral analysis of simulation data, we identify a slow MC-Rossby mode, that follows the dispersion curve predicted by a quasi-geostrophic linear theory. The result indicates that such waves can be excited in the planetary fluid core and that wave propagation may indeed play a role in the magnetic drifts. This gives a framework for further exploration of different wave types, which can provide valuable information about the physical properties in the deep interior fluid core.

A generating process of the geomagnetic drifting field

YUKUTAKE, Takesi^{1*} ; SHIMIZU, Hisayoshi²

¹None, ²Earthquake Research Institute, University of Tokyo

The geomagnetic field is comprised of drifting and standing field. The drifting field is the field that drifts westwards nearly steadily over the past several hundred years and the standing field is that stays at the same place. The drifting field has two major characteristic features. When the field is expressed in a spherical harmonic series, the drifting field mainly consists of sectorial harmonics. Secondly the rate of drift is uniform irrespective of the harmonics. This means the drift velocity is non-dispersive.

We here propose a model of the generating process of the drifting field. Because of the non-dispersive nature of the drift velocity, we assume the westward drift is a phenomenon closely tied with material flow rather than a magnetohydrodynamic wave. Furthermore we take it a phenomenon near the surface of the core where the dipole field is dominant.

If the mantle is approximated by an electrical insulator, the electric current in the core normal to the core-mantle boundary must be zero. This provides a strong constraint on the liquid flow near the surface. If we assume infinite conductivity of the core for simplicity, only the sectorial flow is allowed for the toroidal flow, and the meridional flow for the poloidal flow. The sectorial toroidal flow, interacting with the dipole field, induces sectorial poloidal field, whereas the meridional poloidal flow produces the meridional poloidal field. The surface layer, which is rotating westwards as a whole, carries these fields westwards together. Since the rotation of the meridional field is unrecognizable, only the sectorial field is observed as the drifting field.

We present a simplified model that describes the above process.

Keywords: geomagnetic secular variation, westward drift, drifting field, core surface flow

Electrical resistivity of hcp-Fe under Earth's core conditions

OHTA, Kenji^{1*}; KUWAYAMA, Yasuhiro²; HIROSE, Kei³; OHISHI, Yasuo⁴

¹Department of Earth and Planetary Sciences, Tokyo Institute of Technology, ²Geodynamics Research Center, Ehime University, ³Earth-Life Research Institute, Tokyo Institute of Technology, ⁴Japan Synchrotron Radiation Institute

Iron is the primary component of the Earth's core. Convection of the conductive liquid outer core generates the geomagnetic field, and secular cooling of the core induces growth of the solid inner core and dynamics in the Earth's inside. Synchrotron x-ray diffraction study suggests that iron crystallizes in the hexagonal close-packed structure at the inner core conditions (Tateno et al., 2010). Thus, the electrical resistivity of hexagonal close-packed iron (hcp-Fe) is a key piece of information for estimating the transport properties of the core. We report high temperature electrical resistivity for hcp-Fe to 185 GPa measured in a laser-heated diamond anvil cell. We observed resistivity saturation in hcp-Fe under high pressure and high temperature conditions as predicted in a recent laboratory-based model for the conductivity of the Earth's core (Gomi et al., 2013). The saturation effect is significant in estimating electrical and thermal conductivity of the core, which strongly affect the dynamics and thermal evolution of the Earth.

References

Gomi, H. et al. The high conductivity of iron and thermal evolution of the Earth's core. *Phys. Earth Planet. Inter.* 224, 88-103 (2013).

Tateno, S., Hirose, K., Ohishi, Y., & Tatsumi, Y. The structure of iron in Earth's inner core. *Science* 330, 359-361 (2010).

Keywords: Electrical resistivity, Earth's core, hcp iron

Spatial dependence of anisotropic thermal diffusivity and its influence on dynamics in the Earth's core

MATSUSHIMA, Masaki^{1*}

¹Tokyo Institute of Technology

Small-scale fluid motions in the Earth's core are likely to be highly anisotropic because of rapid rotation of the Earth and a strong magnetic field in the core. We have carried out direct numerical simulations of rotating magnetoconvection to investigate the effect of anisotropic diffusivity on dynamics in the Earth's core, as one of pilot studies. When a computational region is expressed in terms of a rectangular box with periodic boundaries in the three-directions, the prescribed anisotropic thermal diffusivities were found not to influence the character of rotating magnetoconvection, such as kinetic and magnetic energies averaged over the computational region. When a computational region is expressed in terms of a rectangular box with rigid boundary surfaces perpendicular to the gravitational direction, the prescribed anisotropic thermal diffusivities have a significant effect on the character of rotating magnetoconvection; that is, kinetic and magnetic energies can be increased even by a small anisotropy. The degree of increase depends on the direction of anisotropy and the direction of gravity corresponding to location of the computational region. These results suggest that anisotropic thermal diffusivity insignificantly influences dynamics in the bulk of the core, but that it should be effective near rigid boundary surfaces. Therefore, it is likely that anisotropic diffusivity has a more significant effect on MHD dynamos in rotating thin spherical shells. Such an implication can be examined through global numerical simulations of MHD dynamo models with anisotropic diffusivity being variable in the core.

Instead of such a study, we perform further direct numerical simulations of rotating magnetoconvection by prescribing anisotropic thermal diffusivities with spatial dependence; for example, in one case, anisotropic thermal diffusivities are presumed to be effective only near rigid boundary surfaces; in another case, anisotropic thermal diffusivities are presumed to be effective only far from rigid boundary surfaces. Hence this is another pilot study. Kinetic and magnetic energies in the former case seem to be larger than those in the latter case. The result is consistent with that obtained in our previous studies.

Keywords: anisotropic thermal diffusivity, core dynamics

Can a stably stratified layer interrupt the top-down dynamics of Earth's core?

NAKAGAWA, Takashi^{1*}

¹IFREE, JAMSTEC

Takashi Nakagawa

In some of previous studies of numerical dynamo simulation with a stably stratified region below the outer boundary, the long-wavelength feature of radial magnetic field can be only found on the outer boundary because a stratified layer can filter small-scale features of radial magnetic field generated in the convective region below the stratified boundary [Christensen, 2006; Nakagawa, 2011]. The existence of the stably stratified region below the core-mantle boundary (CMB) is recently exposed from high pressure mineral physics [e.g. Pozzo et al., 2012] and seismological data analysis [e.g. Helffrich and Kaneshima, 2013].

Regarding the modeling on geomagnetic secular variation from numerical dynamo simulations, the heterogeneous thermal/chemical anomalies at the core-mantle boundary is important for understanding the time-scale of secular variation such as polarity reversals and excursions suggested from paleomagnetic observations [e.g. Olson et al., 2011; Olson et al., 2013] and current observational magnetic field [Aubert et al., 2013]. However, their investigation was not included in the effects of the stably stratified region below the CMB in their dynamo simulations.

Here we introduce several examples of numerical dynamo simulations with both heterogeneous outer boundary prescribed by the CMB heat flux calculated from numerical mantle convection simulations and a stably stratified layer. Preliminary results are found that the large-scale and amplitude of thermal/chemical anomalies induced by the heterogeneous boundary condition, that is, thermal wind type flow, may be trapped at the imposed stratified boundary. This may imply that the geomagnetic secular variations related to the core-mantle coupling may be suggested that the core surface flow would be a key physics.

Keywords: Earth's core, heterogeneity, core-mantle boundary, stably stratified layer, thermal wind

Sound velocity measurements of liquid Fe-Ni-S alloy at high pressure and temperature via inelastic X-ray scattering

IMADA, Saori^{1*} ; NAKAJIMA, Yoichi² ; KOMABAYASHI, Tetsuya³ ; HIROSE, Kei⁴ ; TSUTSUI, Satoshi⁵ ; UCHIYAMA, Hiroshi⁵ ; ISHIKAWA, Daisuke⁵ ; ALFRED, Baron²

¹Department of Earth and Planetary Sciences, Tokyo Institute of Technology, ²Material Dynamics Laboratory, RIKEN SPring-8 Center, RIKEN, ³School of Geosciences, The University of Edinburgh, ⁴Earth-Life Science Institute, Tokyo Institute of Technology, ⁵Japan Synchrotron Radiation Research Institute

The liquid Earth's outer core is mainly composed of Fe-Ni alloy with some amounts (5~10%) of light element(s), such as hydrogen, carbon, oxygen, silicon, and sulfur. Moreover, it has been known that the Mars and Mercury have also liquid (outer) core, although there are less observational data (Dehant, 2003, Margot et al., 2007).

In order to identify the kind and amount of the light elements dissolved in these planetary cores, sound velocity data of iron alloys at high pressure and temperature are important because the seismic wave speeds are the primary observed information in the deep Earth's interior. While sound velocity measurements of solid core materials up to core pressures have been extensively conducted via ultrasonic method, inelastic X-ray scattering (IXS), nuclear resonance IXS, due to its experimental difficulty, there exist few reports on sound velocity measurements of liquid Fe alloys at high pressure (Nishida et al. 2012).

We measured sound velocity of liquid of (Fe,Ni)₃S up to 30 GPa. Sulfur has been considered to be a major candidate for the light element in the Earth's outer core as well as in the Martian and Mercury's cores (e.g. Lodders and Fegley 1997). We conducted high-pressure and -temperature experiments with an externally-heated diamond-anvil cell (EHDAC). The starting materials were a synthesized or a powder mixture of Fe, Ni, and FeS, with compositions of (Fe_{0.83}Ni_{0.17})₃S, or (Fe_{0.64}Ni_{0.36})₃S. Sound velocity was measured using high resolution IXS at BL35XU, or BL43XU of SPring-8. IXS spectra were collected in the range of the momentum transfer, $Q=3.2\text{?}6.59\text{ nm}^{-1}$ with a resolution of 0.45 nm^{-1} . EHDAC was put in a vacuum chamber to reduce the background of the spectra. We will present the sound velocity data of liquid and solid of (Fe,Ni)₃S and discuss the composition of the terrestrial, Martian, and Mercury's liquid outer core.

Keywords: sound velocity, inelastic X-ray scattering, planetary outer core, liquid iron alloy, High-PT experiment

Experimental approach to the core-mantle boundary region of Mercury

OKAMOTO, Miho¹ ; URAKAWA, Satoru^{1*}

¹Dept Earth Sci, Okayama Univ

MESSENGER mission revealed precise moment of inertia parameters of Mercury and its surface chemistry [1, 2]. These data allow to model the internal structure of Mercury, which has a large liquid core with ~2000 km radius and a solid outer shell with ~400 km thickness [3, 4]. As density of solid outer portion is apparently higher than that of the expected mantle silicate, the solid outer layer must include dense materials. Recent models [3, 4] showed that the Mercury's core contains sulfur and silicon as light elements due to high S fugacity and low oxygen fugacity of its interior. Those models presented a solid FeS layer at bottom of solid outer shell of Mercury as a dense layer, which separated from liquid outer core as a FeS-rich liquid due to liquid immiscibility of the Fe-S-Si ternary system. To investigate the FeS-rich layer at the top of Mercury's core, we performed the high-pressure experiments on the Fe-S-Si system using a KAWAI-type multi-anvil apparatus.

Pressure is fixed at 5 GPa corresponding to the CMB of Mercury and temperature is 1800 K, which is 200 K above the liquidus of Fe-S-Si system reported by Sanloup and Fei [5]. Fe-S-Si sample was kept for 30 min at this condition, and then it was quenched into room temperature. Oxygen fugacity of run charges was maintained around 3 log unit below IW buffer. Texture and chemistry of recovered samples were examined by electron microprobe.

We found two immiscible liquids in one run charge, which consist of Fe,Si-rich metallic liquid and FeS-rich sulfide liquid. Sulfur content of metallic liquid ranges 6 to 9 at%, which is higher by ~5 at% than those reported by Morard and Katsura [6]. Differences in texture of recovered samples and run duration between this study and Morard and Katsura [6] suggest that the latter experiments were in disequilibrium state. Our data shows the liquid immiscible region has a narrower extent than the previous estimation and the Mercury immiscible Fe-S-Si core must contain at least 6-9 at% sulfur. The quenched FeS-rich liquid phase consists mainly of crystalline FeS (~90 vol%) and Fe-Si alloy. In the case that FeS-rich liquid contacted with MgO sample container, (Mg_{0.8}Fe_{0.2})S crystalline phase coexisted with FeS-rich liquid. Mg-sulfide phase could be made by Fe-Mg exchange reaction between MgO and FeS-rich liquid. In the Mercury core, when FeS-rich liquid ascends to add the bottom of the CMB due to its buoyancy, it makes a stable low density layer. Mg-sulfide phase is produced under low oxygen fugacity and high sulfur fugacity at CMB, and then it incorporates into mantle. This is consistent with the results of X-ray fluorescence spectrometry on the Mercury's surface, which indicates the presence of Mg and Ca sulfides [2].

References

- [1] Margot JL et al., J. Geophys. Res., 117, E00L09, 2012.
- [2] Nittler LR et al., Science, 333, 1847, 2011.
- [3] Smith DE et al., Science, 336, 214, 2012.
- [4] Hauck II SA et al., J. Geophys. Res.: Planets, 118, 1204, 2013.
- [5] Sanloup C and Fei Y, Phys. Earth Planet. Inter., 147, 57, 2004.
- [6] Morard G and Katsura T, Geochim. Cosmochim. Acta, 74, 3659, 2010.

Keywords: core, CMB, Mercury